International Journal of Microwave and Wireless Technologies

cambridge.org/mrf

Compact multiband cuff button antenna for WBAN application

Sapna Bijimanzil Abdulkareem and Ramasamy Kuppusamy

Department of Electronics and Communication Engineering, KIT-Kalaignarkarunanidhi Institute of Technology, Coimbatore, Tamil Nadu, India

Research Paper

Cite this article: Bijimanzil Abdulkareem S, Kuppusamy R (2024) Compact multiband cuff button antenna for WBAN application. *International Journal of Microwave and Wireless Technologies* **16**(10), 1739–1748. https://doi.org/10.1017/S1759078724001223

Received: 6 May 2024
Revised: 12 November 2024
Accepted: 13 November 2024

Keywords:
button antenna; multiband; Low SAR; WBAN

Corresponding author:
Sapna Bijimanzil Abdulkareem;
Email: sapna_psmi@yahoo.co.in

Abstract

A compact dual layer conformal wearable quad band antenna is proposed for wireless body area network applications. The proposed button like patch antenna resonates at 2.5 GHz (industrial, scientific, and medical bands)/3.6 GHz sub six 5G band/5.75 GHz (wireless local area network/ISM band)/ and 9.8 GHz (X band) frequencies. The circular textile antenna is constructed with jean and polydimethylsiloxane substrate having a slotted ground of radius 10 mm and thickness 1.5 mm. The simulated gains obtained at the operating bands are 1.85/2.03/1.49/3.27 dBi, respectively. The designed antenna's directed radiation pattern assures reduced backward radiation to body tissue. The specific absorption rate (SAR) analysis for the antenna at multiple resonant frequencies has also been reported, which are well below the SAR threshold of 1.6 W/kg for 1 gm of tissue, indicating that the model works adequately for wearable applications. The experimental characterization on- and off-body of the fabricated antenna validates the simulated results.

Introduction

Rapid technological advancement in the field of wireless body area networks (WBAN) paved the way for multiple real time applications including health care industry, emergency rescue, defense, location tracking, sports, and physical fitness etc. WBAN enables either on-body or off-body communication in which information can be communicated between devices within on the body or to remotely connected devices and servers like in hospital for health care monitoring. WBAN application requires wearable antennas with special features like, comfort, compactness, durability, flexibility, robustness, and higher gain. Body tissues are highly vulnerable to electromagnetic signals, thus wearable or any on-body antenna should have low specific absorption rate (SAR) which can be easily achieved with low back radiation. Extensive research on wearable on-body antennas is performed. Wearable antennas are designed as printed, embroidery or button types in rigid (FR-4) and flexible (Jean, polydimethylsiloxane [PDMS]) substrates to suit the application [1–9]. Antenna performance is evaluated in the presence of water and moisture and shows that textile material has a larger impact on performance degradation on longer life. Rigid materials are long lasting with better performance but not comfortable for wearing. Thus flexible and comfortable substrate like PDMS is always a better equivalent providing good performance. Most applications comply with dual band antenna compared to single band antennas for wireless applications [10–17]. Most dual band wearable antennas operate in 2.4 and 5.8 GHz frequency bands falling in industry, scientific, and medical application. In order to accommodate high data rate and multiple operation frequency Multiple Input Multiple Output (MIMO) and reconfigurable antennas are preferred [18–20]. Miniaturization is another important factor on antenna design, miniaturized antennas with stubs, slots and fractals can improve the number of operating bands with wider bandwidths [21–27]. Pattern and polarization diversity button antennas are suitable for on/off-body applications [28–32]. In wearable antennas button antennas are prominently used as they are easily designed with metallic structures or snap buttons themselves act as radiators with different arrangements to make multiple bands with better performance. Their ease of integration to cloths and comfort of wearing make it as a best choice of wearable antenna for WBAN application.

This paper presents a miniaturized novel circular button antenna with multiple bands using PDMS and jean as the substrate. Full ground plane with an arc minimizes the SAR value with an additional benefit of extra band. Thus the proposed button antenna is compact, flexible, and comfortable to integrate in the blazer or jacket.

Submission

The proposed circular blazer cuff button antenna is designed with 10 mm radius on dual dielectric substrate consisting of 0.5 mm jean at the bottom and a 1 mm PDMS elastomer at

© The Author(s), 2024. Published by Cambridge University Press in association with The European Microwave Association.

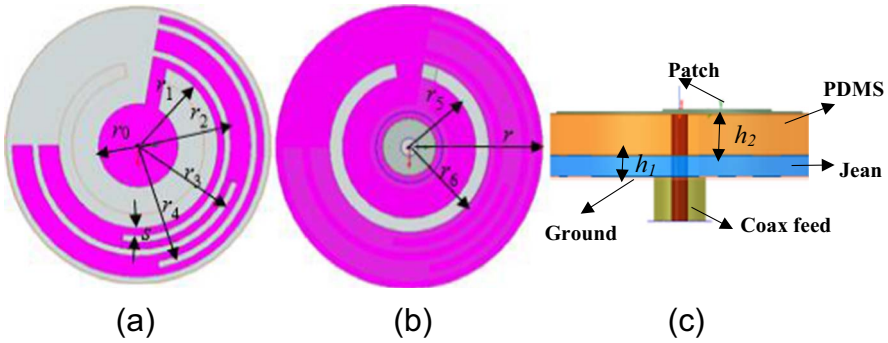


Figure 1. Proposed button antenna (a) Top view (b) Bottom view (c) Side view.

Table 1. Proposed antenna dimensions

Antenna parameter	r	r_0	r_1	r_2	r_3	r_4	r_5	r_6	s	t	h_1	h_2
Value	10	3	6	7	8	9	5	6	0.5	0.05	0.5	1

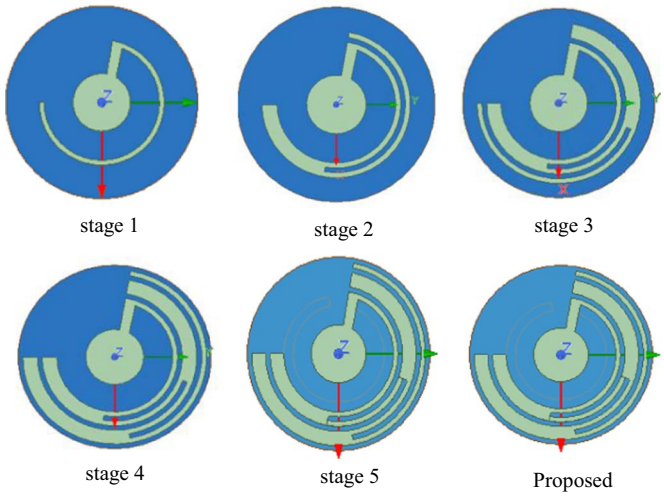


Figure 2. Evolution of cuff button antenna.

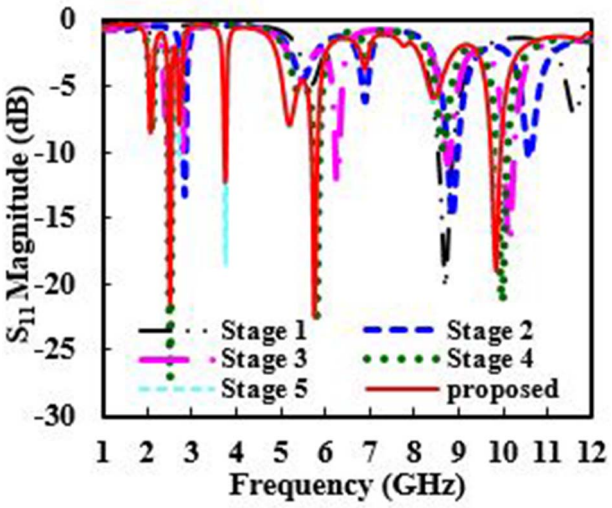


Figure 3. Reflection performance of antenna during evolution.

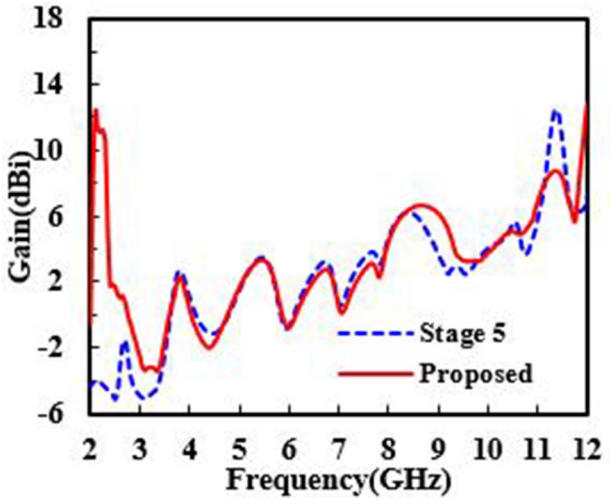


Figure 4. Gain performance of last two antenna stages.

the top. The dielectric permittivity ε of Jean and PDMS substrate are 1.6 and 2.7 with loss tangent tan δ = 0.02 and 0.0314, respectively. The unique geometry consists of a circular conductor and four interconnected arcs with radius $r1$, $r2$, $r3$, and $r4$ from the center which are interconnected to form a single slotted arc geometry. The radiating element of multiple arc section with a circular center attached with a narrow strip is printed on the PDMS substrate. Top, bottom, and side view of the proposed antenna is shown in as shown in Fig. 1. The circular ground conductor with an arc slot acting as the ring resonator is printed on the bottom of the jean substrate. Adhesive is used to connect both copper and substrate materials. The inner and outer radius of the ground slot arc are $r5$ and $r6$. Dimensions of the antenna are tabulated in Table 1. The antenna is fed by a 50 Ω coaxial probe at the center for better impedance match.

Antenna evolution stages

Evolution of antenna geometry in different stages are shown in Fig. 2. Initial geometry has a circular patch with an arc connected through a stub. It resonates at 8.7 GHz with a return loss of 20.29 dB. Additional arc attached to stage 1 contributed with multiple resonances as shown in Fig. 2. Stage 2 resonates at 8.85 GHz frequency and 2.85 GHz frequency with S_{11} respectively as −14.89 and −13.19 dB. Antenna design started with basic expression of patch with radius a as shown in equation (1). Stage 3 also has three resonances at 6.25, 8.75, and 10.1 GHz which are not the

https://doi.org/10.1017/S1759078724001223 Published online by Cambridge University Press

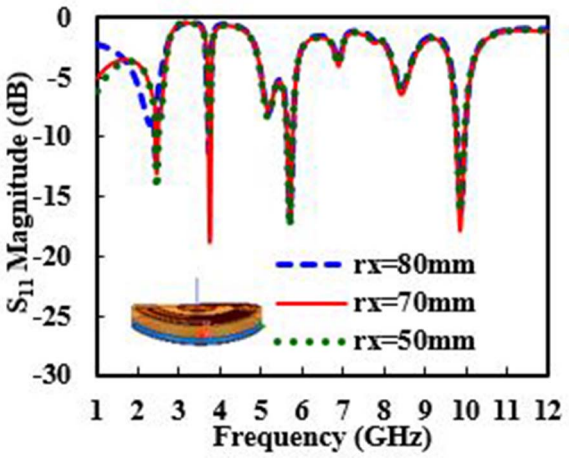


Figure 5. Effect of antenna bending along x axis.

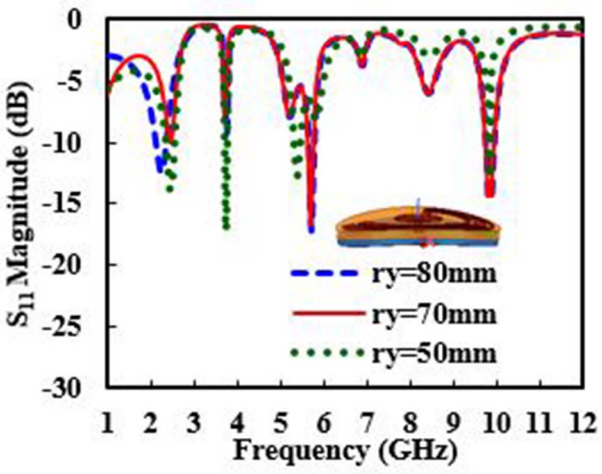


Figure 6. Effect of antenna bending along y axis.

intended frequencies. Addition of 4th strip as in stage 4 achieved resonance at 2.5, 5.8, and 10 GHz with better S_{11} values, −27.03, −22.94, and −21.18 dB. In stage 5 an arc slot is introduced in the ground plane to enable resonance at 3.6 GHz which can be utilized for 5G application.

$$f = \frac{1.8412\, v_0}{2\pi a\sqrt{\varepsilon}} \tag{1}$$

Thus the multiband antenna of stage 5 resonates at four frequencies respectively at 2.5, 3.6, 5.75, and 9.8 GHz suitable for WLAN, WBAN, 5G, and X band applications with return loss of 15.39/18.43/22.19/18.18 dB. All four arc strips have an angle of 260°. The four arcs are interconnected with smaller angular strips. Optimization was performed to for arc lengths to achieve the required resonance. Inner interconnection arc has an angle of 80° and the outer two interconnecting arcs have an angular gap of 100° each. Return loss plots of various stages are in Fig. 3. The antenna with slotted ground had better reflection characteristics with resonance at four frequencies including sub 6, 5G band of 3.6 GHz, but the gain at 2.4 GHz was low showing −5.07 dB. In order to improve further gain at lower frequency an additional strip is attached to the top of 2nd arc. Gain plots of the antenna for last two stages are compared in Fig. 4. The additional stub in the proposed antenna improved the gain at 2.45 GHz from −5.07 to 1.85 dB. All simulations were carried out using HFSS. Flexibility of proposed cuff button antenna is confirmed by bending analysis along X and Y direction as shown in Figs. 5 and 6. The S_{11} plots show stable performance on bending at all four frequency bands. Proposed antenna has lower bandwidth 60 MHz (2.47–2.53 GHz), 30 MHz (3.76–3.73 GHz), 140 MHz (5.83–5.69 GHz), and 220 MHz (9.95–9.73 GHz), respectively due to smaller strip widths. Simulated efficiency of the antenna at operating frequencies of 2.5, 3.75, 5.75, and 9.8 GHz are 84.52%, 86.21%, 77.77%, and 86.18%, respectively. The antenna is tilted in different angles along X and Y direction during simulation and Fig. 7 shows the tilted antenna return loss at 20° in front & back along X axis and left & right along Y axis. The performance of the antenna remains good on tilting.

Current distribution

The surface current distribution of the proposed multilayer multiband cuff button antenna is shown in Fig. 8. Maximum current is for 2.5 GHz and minimum for 9.8 GHz. Coverage of strips is more in case of 5.75 GHz. The current distribution indicates

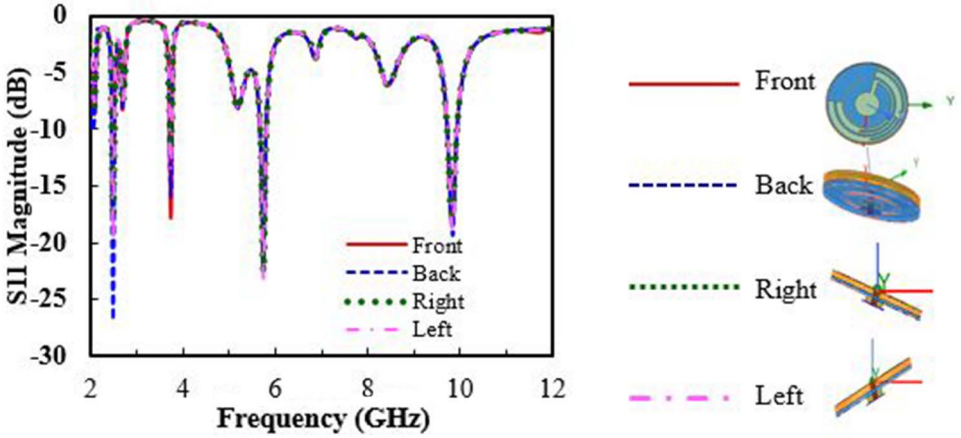


Figure 7. Effects of antenna tilting along X and Y axis at 20° indicating front, back, right, and left.

https://doi.org/10.1017/S1759078724001223 Published online by Cambridge University Press

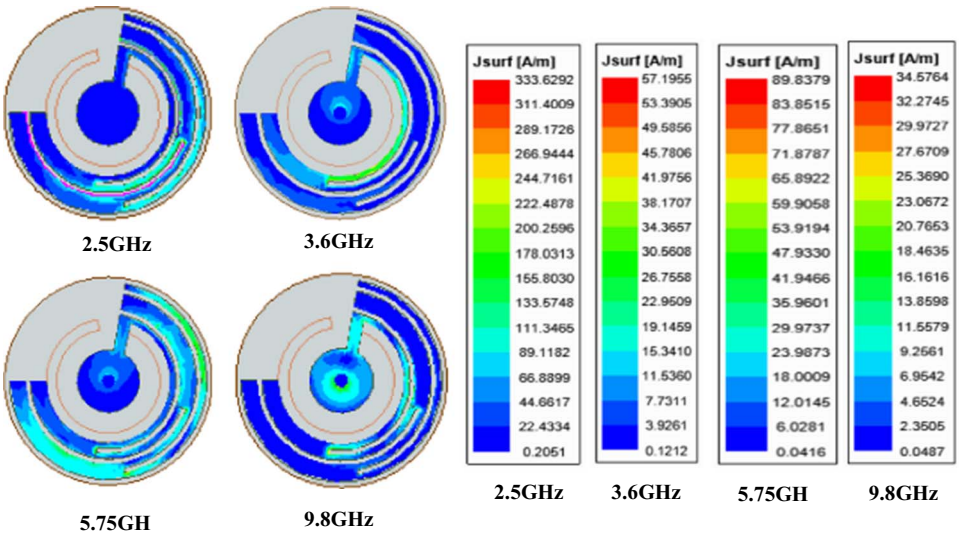


Figure 8. Surface current distribution of the button antenna at resonating frequencies.

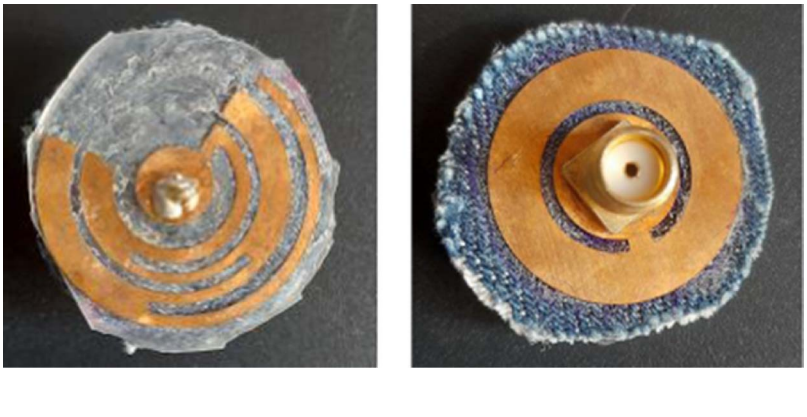


Figure 9. Fabricated cuff button antenna.

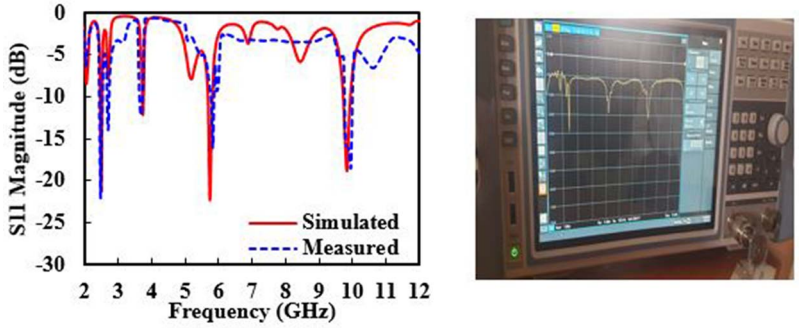


Figure 10. Comparative S_{11} of simulation and measurement with measured photograph.

the strip position responsible for maximum radiation at different frequencies.

Results and discussion

Off-body antenna performance

The prototype of fabricated antenna is shown in Fig. 9. The antenna reflection performance is measured with the help of R&S's Network analyzer ZNLE14 as in Fig. 10 and the results of simulation and measurement shows a close agreement with each other. The measured results indicate resonance at 2.48, 3.69, 5.84, and 9.96 GHz with corresponding S_{11} readings as −22.11, −12.28, −16.08, and −18.40 dB, while simulated return loss was found to be 21.38/12.2/22.41/18.87 dB at frequencies of 2.5, 3.6, 5.75, and 9.87 GHz. Measurements are also carried out placing the antenna at different position on body. Figure 11 depicts the real time return loss performance of the antenna placing on hand and chest in

https://doi.org/10.1017/S1759078724001223 Published online by Cambridge University Press

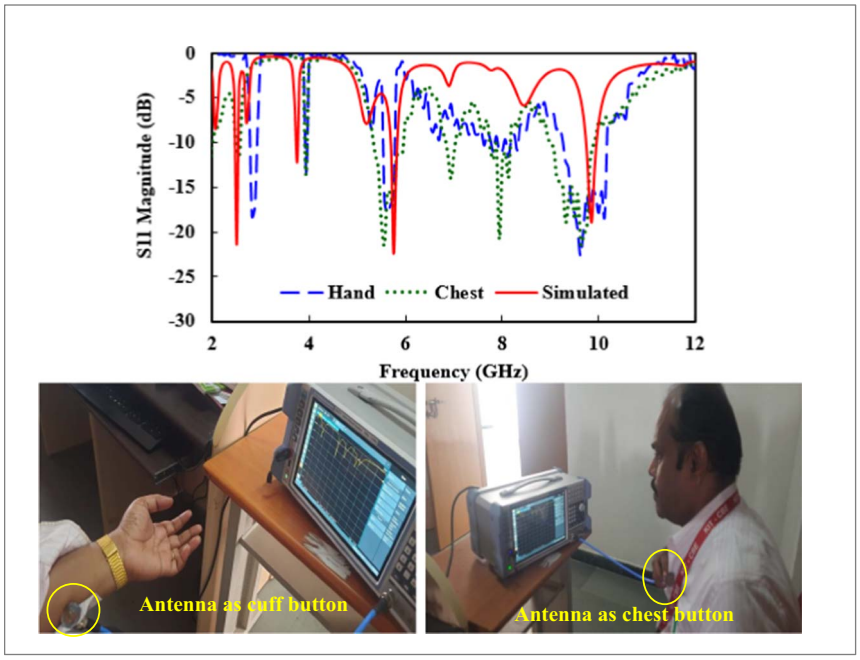


Figure 11. Measured S_{11} performance at different on-body positions.

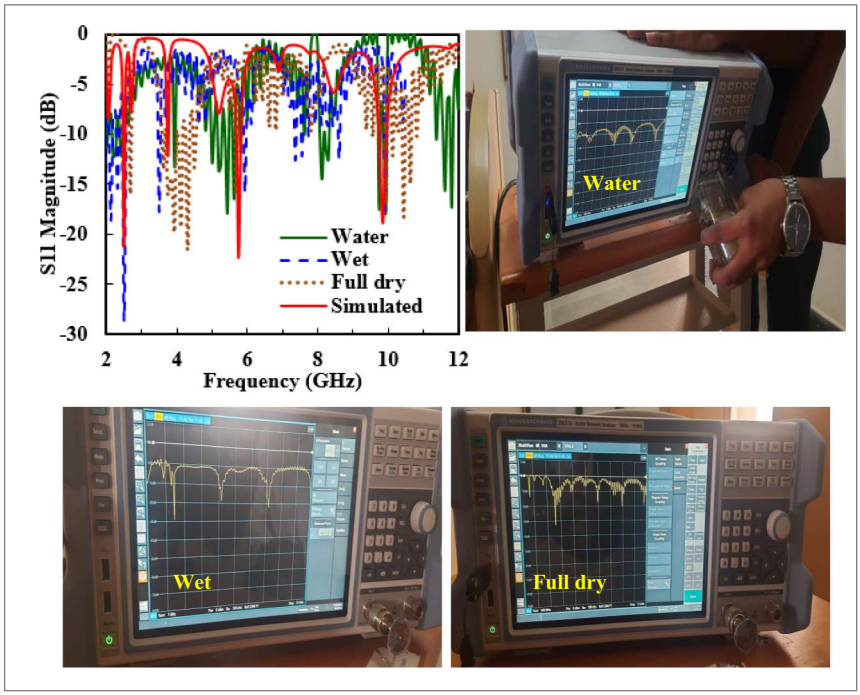


Figure 12. Measured S_{11} performance with water and moisture content.

Table 2. Return loss performance of antenna in different measurement scenario

Analysis setup	Freq. (GHz)	S_{11} (dB)	Freq. (GHz)	S_{11} (dB)	Freq. (GHz)	S_{11} (dB)	Freq. (GHz)	S_{11} (dB)
Simulated	2.5	−21.38	3.6	−12.2	5.75	−22.41	9.87	−18.87
Measured (free space)	2.48	−22.11	3.69	−12.28	5.84	−16.08	9.96	−18.4
In hand	2.8	−18.23	3.94	−13.25	5.63	−17.89	9.94	−17.8
Chest	2.56	−11.48	3.94	−13	5.56	−21.4	9.69	−20.18
Water	2.44	−12.09	3.94	−13.24	5.63	−16.48	9.94	−17.8
Wet	2.5	−28.65	3.5	−17.7	5.94	−15.83	9.94	−17.66
Full dry	2.69	−16	3.94	−19.78	5.69	−15.88	9.94	−16.79

https://doi.org/10.1017/S1759078724001223 Published online by Cambridge University Press

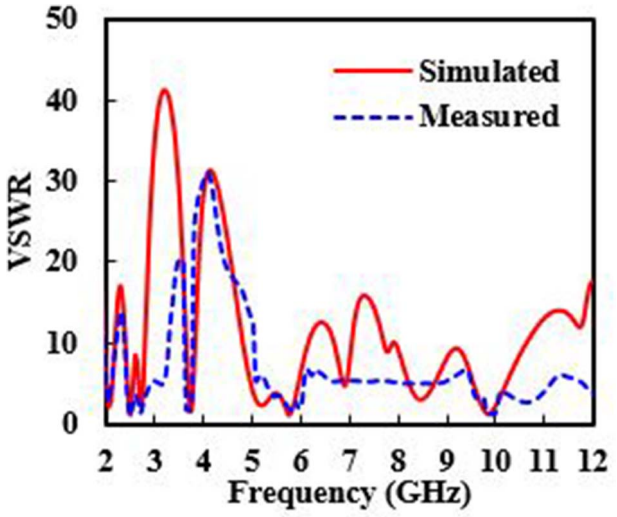


Figure 13. Comparative VSWR of simulation and measurement.

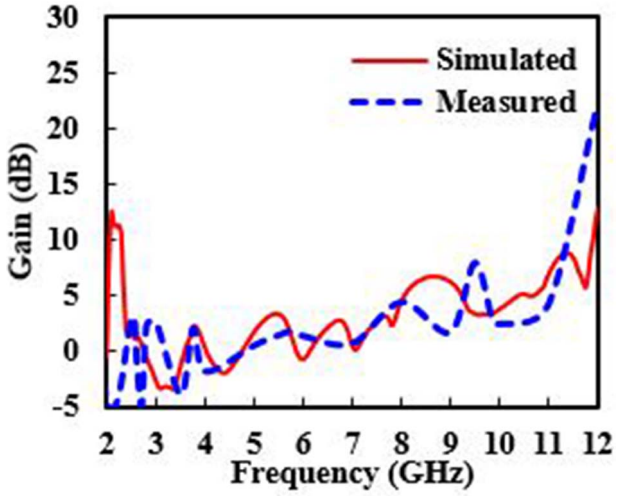


Figure 14. Comparative gain of simulation and measurement.

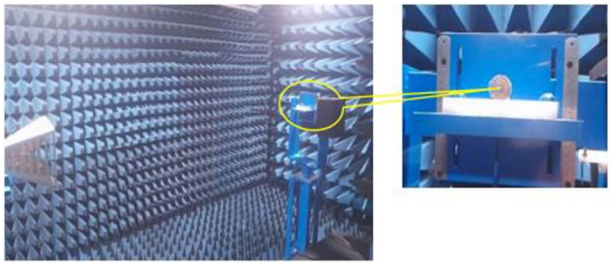


Figure 15. Radiation pattern measurement setup in anechoic chamber.

comparison with simulated result. In order to analyze the water absorption property of jean substrate (wet and moisture condition), the antenna is dipped in water and partially dried and the return loss is measured. Later, when it is fully dried the measurement is repeated to check for any deformity. The results are plotted in Fig. 12. Measured return loss results are tabulated in Table 2. The Voltage Standing Wave Ratio (VSWR) and gain plots of button antennas are depicted in Figs. 13 and 14. VSWR is below 2 for the

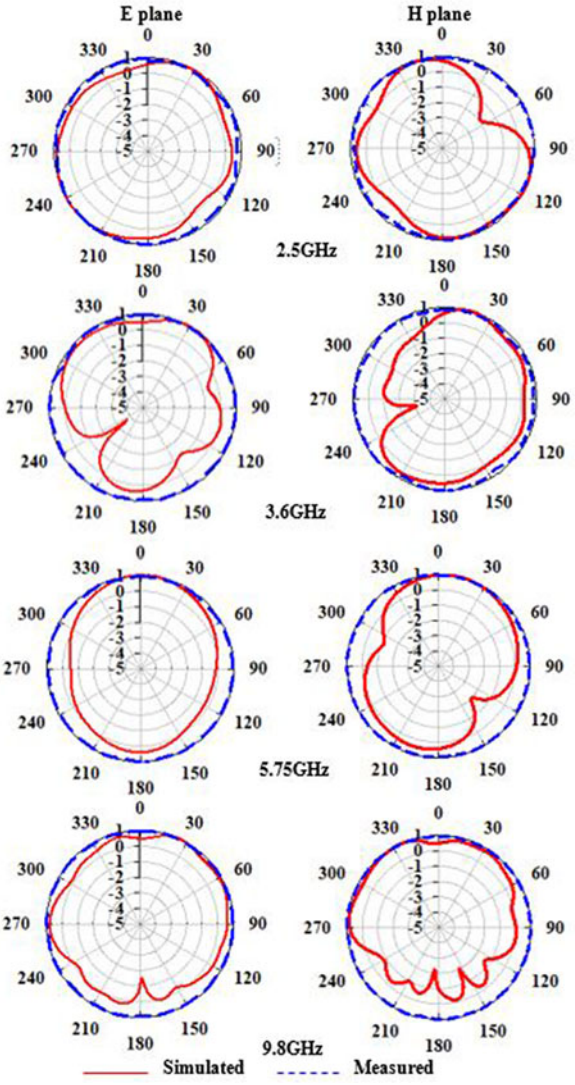


Figure 16. Radiation patterns of cuff button antenna.

resonant frequencies. Measured peak gains at resonance are 3.08, 2.09, 1.79, and 3.03 dB while the simulated gains are 1.85, 2.03, 1.47, and 3.27dB for radiating frequencies.

The radiation patterns in azimuth and elevation plane are measured against 18 GHz rigid horn antenna in an anechoic chamber of size 5 m × 3 m × 2.6 m and the measurements are taken at operating frequencies of 2.5, 3.6, 5.75, and 9.8 GHz which is shown in Fig. 15. Normalized radiation patterns on simulation and measurement in E and H plane are plotted in Fig. 16.

On-body antenna performance

The antenna performance on the body was analyzed by placing it on male right arm with spacing with 2, 5, and 10 mm. Figure 17 show the return loss performance of the antenna at different spacing and resonance frequency. When the antenna is placed at 2 mm distance the lowest two resonances have poor S_{11} magnitude of −9.25 and −6.94 dB at 2.6 and 3.65 GHz. At 5 and 10 mm distance all four bands show S_{11} readings below −10 dB reference. Resonance frequencies and corresponding

https://doi.org/10.1017/S1759078724001223 Published online by Cambridge University Press

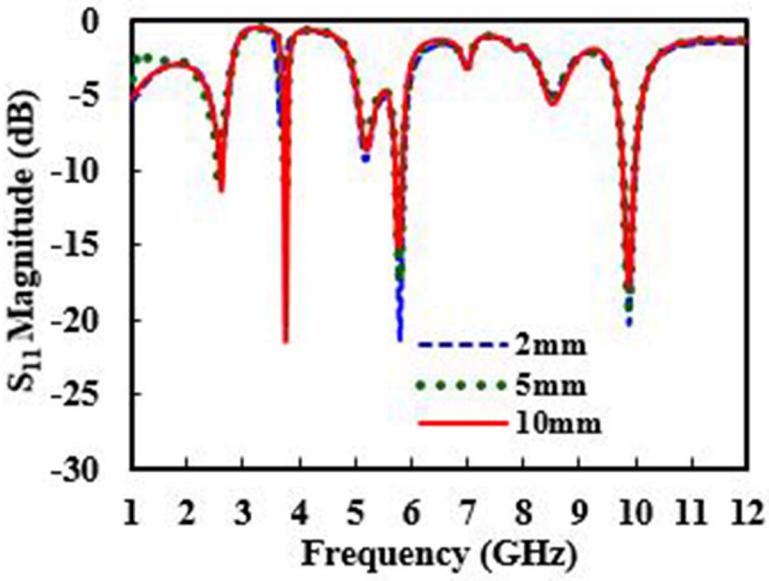


Figure 17. On-body reflection performance of antenna.

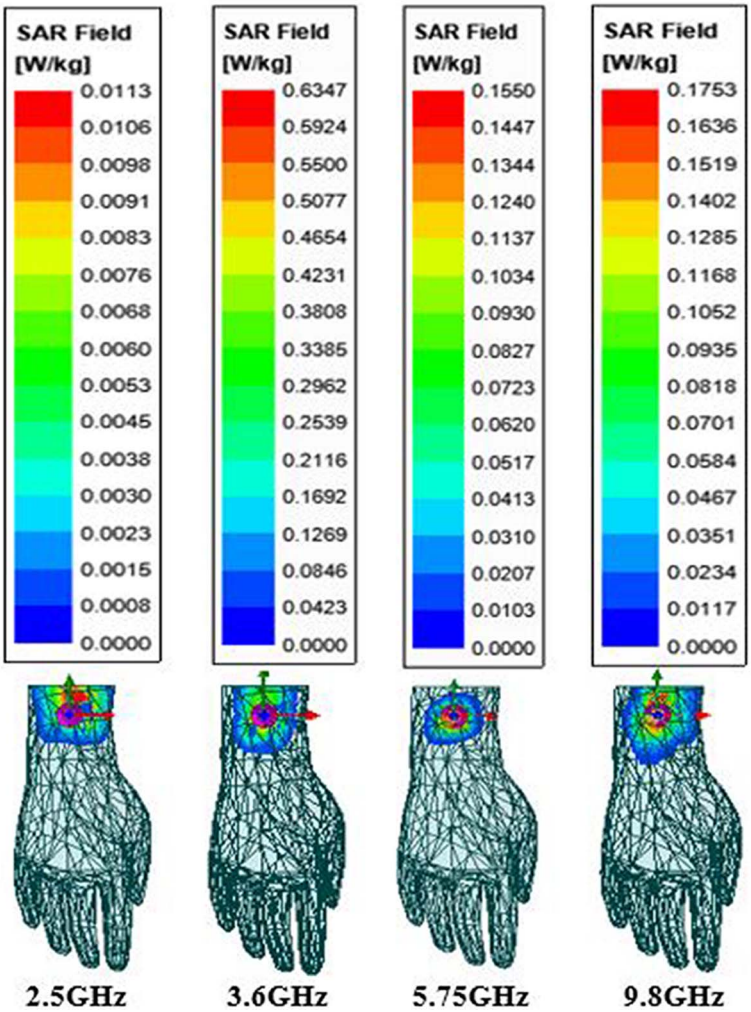


Figure 18. SAR analysis of proposed antenna.

S_{11} magnitude at 5 mm distance are 2.55/3.75/5.8/9.9 GHz & 10.94/11.28/17.34/19.68 dB and at 10 mm distance the S_{11} values are 11.34/21.42/15.07/17.66 dB at 2.6/3.75/5.8/9.9 GHz. This indicates that the on-body dielectric variation has a tendency of smaller frequency shift with reduced S_{11} value when placed close to the body.

https://doi.org/10.1017/S1759078724001223 Published online by Cambridge University Press

Table 3. Comparison with existing literature

Ref. No	Volume (mm^3)	Frequency (GHz)	Bands (GHz)	Radiator	Substrate	Gain (dBi)	SAR
13	6983.2	3.5, 5.8	NA	4 × 4 AMC backed CPW Monopole	Rogers ULTRALAM 3850 substrate,	2.26,3.96 (with AMC 9.3,6.6)	0.903, 0.338 (AMC 0.068, 0.33)
14	12,312	2.45, 5.8	NA	Spiral inverted-F button antenna	Rogers 4003	−0.6 and 4.3	0.39, 0.584 W/Kg for 1 g of tissue
15	31,700	5.5	5.47–5.725	Button	FR-4 & textile	4	NA
17	1739.629976	2.4, 5.6	NA	Slotted patch button	Polytetrafluoroethylene PTFE Taconic ceramic substrate	1.5	NA
19	10,560	2.45, 5.8	2.10–2.05 & 5.63–5.34	Snap button	Rogers RT/Duroid	2.7,7.9	NA
21	84.78	0.867, 2.38, and 5.8	0.852–0.890, 2.35–2.40, and 5.725–5.875	Circular slotted patch button	Rogers RO4003	2.5,3.52&4.8	0.258, 0.57, 0.932
22	15,000	1.8, 2.4, 5.4		Circular patch	RT Duroid 5870	5.5,7.8,7.9	NA
24	9800	1.8, 2.4, 3.6, & 5.5	1.70–2.01, 2.39–2.50, 3.59–3.70, & 5.41–5.65	Circular slotted patch	Polyester cloth	13.1,6.63,3.76,& 6.11	0.274, 1.065, 2.137, and 2.374 W/Kg for 10 g of tissue
25	8524.4	0.9, 1.9, & 2.45		Embroidering	e-fiber textiles	2	NA
26	1017.6	2.4, 3.5,4.4, 5.2, and 5.8	2.33–2.45, 3.24–3.75, 4.24–4.61, 5.13–5.43, and 5.76–5.87	CPW meander lines	RT5880 Duroid	0.64 to 4.94	0.531, 0.593, 0.683, 0.799, 0.998 W/Kg for 1 g of tissue
27	463.01184	4.33, 7.51, 9.31	4.1–4.64 GHz, 7.19–8.03 GHz, and 8.85–9.67	Circular patch	FR4	4.9,3.04 &4.52	0.00155, 0.00125, & 0.0156 W/Kg for 10 g of tissue
Proposed	471	2.5, 3.6, 5.75, & 9.8	2.47–2.53, 3.76–3.73, 5.83–5.69, & 9.95–9.73	Arc button	PDMS & Jean	1.85,2.03,1.49 & 3.27	0.011, 0.634, 0.155, & 0.0175 W/Kg for 1 g of tissue

Antenna SAR analysis

SAR is the amount of radiation absorbed by the body tissues on sensing of electromagnetic radiation. As per the regulatory standards by Federal Communication Commission (FCC), SAR is limited to have a protective environment from radiation hazards with a limit of 1.6 W/Kg for 1 g of tissue or 2 W/Kg for 10 gm of tissue. In this study, human arm phantom is considered for SAR analysis as the antenna is designed to place on the sleeves. The simulation is carried out with 1 g of tissue with an input signal power of 100 mW and 5 mm gap from the body. The evaluated SAR distribution at different frequency are plotted in Fig. 18. SAR value of designed antenna is minimum (0.0113 W/Kg) at 2.5 GHz and maximum (0.6347 W/Kg) at 3.6 GHz. Simulated SAR values at 5.75 and 9.8 GHz frequency are found to be 0.155 and 0.175 W/Kg. Figure 18 clearly shows that the proposed antenna provides a SAR of acceptable FCC limit suitable for safe on-body application. Table 3 show comparison results of the proposed antenna with few existing literatures.

Conclusion

In this article, a miniaturized cuff button antenna is presented for off-body communication for medical application. The multiband antenna covers application frequency bands of 2.5, 3.6, 5.75, and 9.8 GHz with corresponding bandwidth of 60/30/140/220 MHz. The radiation patterns are directional with better gain suitable for real time on-body and off-body communication. The designed miniaturized cuff button antenna has low SAR values and make comfortable for wearable biomedical application.

Acknowledgements. This work was supported by All India Council for Technical Education, under research promotion scheme. File No.8-122/FDC/RPS/POLICY-1/2021-2022.

https://doi.org/10.1017/S1759078724001223 Published online by Cambridge University Press

Competing interests. The authors declare that they have no conflict of interest.

References

1. **Paradiso R, Loriga G and Taccini N** (2005) A wearable health care system based on knitted integrated sensors. *IEEE Transactions on Information Technology in Biomedicine* **9**(3), 337–344.
2. **Zhang L, Wang Z and Volakis JL** (2012) Textile antennas and sensors for body-worn applications. *IEEE Antennas and Wireless Propagation Letters* **11**, 1690–1693.
3. **Paul DL, Giddens H, Paterson MG, Hilton GS and McGeehan JP** (2013) Impact of body and clothing on a wearable textile dual band antenna at digital television and wireless communications bands. *IEEE Transactions on Antennas and Propagation* **61**(4), 2188–2194.
4. **Toivonen M, Björninen T, Sydänheimo L, Ukkonen L and Rahmat-Samii Y** (2013) Impact of moisture and washing on the performance of embroidered UHF RFID tags. *IEEE Antennas and Wireless Propagation Letters* **12**, 1590–1593.
5. **Sanz-Izquierdo B and Batchelor JC** (2007) Button antennas for wearable applications. In *IET Seminar on Antennas and Propagation for Body-Centric Wireless Communications*. London, 97–104.
6. **Chen SJ, Kaufmann T, Ranasinghe DC and Fumeaux C** (2016) A modular textile antenna design using snap-on buttons for wearable applications. *IEEE Transactions on Antennas and Propagation* **64**(3), 894–903.
7. **Floc'h JM, Queudet F and Fourn E** (2007) Radio-electric characterizations of jeans buttons. In *The Second European Conference on Antennas and Propagation, EuCAP 2007*, Edinburgh, 1–4.
8. **Kanemoto M, Yoshida K, Nishimura F, Nishikawa H, Tanaka A and Douseki T** (2020) Ultrasmall-button-shaped rectifier module tied with conductive-yarn antenna for wearable accessories powered by microwaves. In *IEEE Wireless Power Transfer Conference (WPTC)*, Seoul, Korea (South), 349–352.
9. **Sayem ASM, Simorangkir RBVB, Esselle KP, Hashmi RM and Liu H** (2020) A method to develop flexible robust optically transparent unidirectional antennas utilizing pure water, PDMS, and transparent conductive mesh. *IEEE Transactions on Antennas and Propagation* **68**(10), 6943–6952.
10. **Le TT and Yun T-Y:** (2020) Miniaturization of a dual-band wearable antenna for WBAN applications. *IEEE Antennas and Wireless Propagation Letters* **19**(8), 1452–1456.
11. **Wong KL, Chang HJ, Wang CY and Wang SY** (2020) Very-low-profile grounded coplanar waveguide-fed dual-band WLAN slot antenna for on-body antenna application. *IEEE Antennas and Wireless Propagation Letters* **19**(1), 213–217.
12. **Le TT and Yun T-Y** (2021) wearable dual-band high-gain low-SAR antenna for off-body communication. *IEEE Antennas and Wireless Propagation Letters* **20**(7), 1175–1179.
13. **El Atrash M, Abdalla MA and Elhennawy HM** (2019) A wearable dual-band low profile high gain low SAR antenna AMC-backed for WBAN applications. *IEEE Transactions on Antennas and Propagation* **67**(10), 6378–6388.
14. **Zhang XY, Wong H, Mo T and Cao YF** (2017) Dual-band dual-mode button antenna for on-body and off-body communications. *IEEE Transactions on Biomedical Circuits and Systems* **11**(4), 933–941.
15. **Xiaomu H, Yan S and Vandenbosch GAE** (2017) Wearable button antenna for dual-band WLAN applications with combined on and off-body radiation patterns. *IEEE Transactions on Antennas and Propagation* **65**(3), 1384–1387.
16. **Salman LKH and Talbi L** (2010) Dual band G-shape wearable cuff button antenna for ISM bands applications. In *IEEE Antennas and Propagation Society International Symposium*, Toronto, ON, Canada, 1–4.
17. **Sreelakshmy R and Vairavel G** (2019) Novel cuff button antenna for dual-band applications. *ICT Express* **5**(1), 26–30.
18. **Kumar Biswas A, Pattanayak SS and Chakraborty U** (2020) Evaluation of dielectric properties of colored resin plastic button to design a small MIMO antenna. *IEEE Transactions on Instrumentation and Measurement* **69**(11), 9170–9177.
19. **Chen SJ, Ranasinghe DC and Fumeaux C** (2018) A robust snap-on button solution for reconfigurable wearable textile antennas. *IEEE Transactions on Antennas and Propagation* **66**(9), 4541–4551.
20. **Dang QH, Chen SJ, Ranasinghe DC and Fumeaux C** (2021) A frequency-reconfigurable wearable textile antenna with one-octave tuning range. *IEEE Transactions on Antennas and Propagation* **69**(12), 8080–8089.
21. **Sambandam P, Kanagasabai M, Natarajan R, Alsath MGN and Palaniswamy S** (2020) Miniaturized button-like WBAN antenna for off-body communication. *IEEE Transactions on Antennas and Propagation* **68**(7), 5228–5235.
22. **Parveen T, Khan QU, Fazal D, Ali U and Akhtar N** (2019) Design and analysis of triple band circular patch antenna. *AEU - International Journal of Electronics and Communications* **12**, 152960.
23. **Lai J, Wang J, Sun W, Zhao R and Zeng H** (2022) A low profile artificial magnetic conductor based tri-band antenna for wearable applications. *Microwave and Optical Technology Letters* **64**, 123–129.
24. **Danvir M and Pattnaik SS** (2018) Quad-band wearable slot antenna with low SAR values for 1.8 GHz DCS, 2.4 GHz WLAN and 3.6/5.5 GHz WiMAX applications. *Progress in Electromagnetics Research B* **81**, 163–182.
25. **Wang Z, Lee LZ, Psychoudakis D and Volakis JL** (2014) embroidered multiband body-worn antenna for GSM/PCS/WLAN communications. *IEEE Transactions on Antennas and Propagation* **62**(6), 3321–3329.
26. **Dey AB, Mitra D and Arif W** (2020) Design of CPW fed multi-band antenna for wearable. *International Journal of RF and Microwave Computer-Aided Engineering* **30**(12), e22459.
27. **Dash RK, Saha PB, Ghoshal D and Palai G** (2023) Fractal slot loaded compact wearable button antenna for IOT and X-band applications. *Wireless Networks* **29**, 589–605.
28. **Zhou L, Fang S and Jia X** (2020) Dual-band and dual-polarised circular patch textile antenna for on-/off-body WBAN applications. *IET Microwaves, Antennas & Propagation* **14**, 643–648.
29. **Zhang J, Yan S, Hu X and Vandenbosch GAE** (2019) Dual-band dual-polarized wearable button array with miniaturized radiator. *IEEE Transactions on Biomedical Circuits and Systems* **13**(6), 1583–1592.
30. **Le TT, Kim Y-D and Yun TY** (2022) Wearable pattern-diversity dual-polarized button antenna for versatile on-/off-body communications. *IEEE Access* **10**, 98700–98711.
31. **Yin X, Chen SJ and Fumeaux C** (2020) Wearable dual-band dual-polarization button antenna for WBAN applications. *IEEE Antennas and Wireless Propagation Letters* **19**(12), 2240–2244.
32. **Hu X, Yan S and Vandenbosch GAE** (2019) Compact circularly polarized wearable button antenna with broadside pattern for U-NII worldwide band applications. *IEEE Transactions on Antennas and Propagation* **67**(2), 1341–1345.



Sapna B A obtained her B.E. in electronics and communication engineering from Madras University, India in 2000, an M.E. in communication systems in 2007, and Ph.D. in Electronics and Communication Engineering in 2022 from Anna University, India. She is working as an assistant professor at KIT-Kalaignar Karunanidhi Institute of Technology, Coimbatore, India. She is a life member of ISTE. Her research interests include planar antennas, wearable antennas, implantable antennas frequency-selective surface (FSS), and metamaterials.

https://doi.org/10.1017/S1759078724001223 Published online by Cambridge University Press



K. Ramasamy obtained B.E. ECE from Madurai Kamaraj University, M.E. applied electronics from Bharathiar University, India, and Ph.D. communication engineering from Multimedia University, Malaysia, in 1988, 1993, and 2006, respectively. He is a fellow in IETE, and member in ISTE. He has more than 35years of experience in academics and administration in different engineering colleges in India and abroad. Currently, he is professor and dean Academics and Research at Kalaignar Karunanidhi Institute of Technology, Coimbatore. He published around 150 papers and his research interests include design of microstrip antennas and wireless communication. He guided three Ph.D. scholars. He is a recipient of National Merit Scholarship Award by Government of India, and EMC^2 Academic Leader Award 2015, also awarded the silver medal in KERIE 2006, conducted by Faculty of Engineering, International Islamic University Malaysia, for best Ph.D. work Asymmetric Turbo Code for Enhanced Performance of JPEG Coded Image Transmission over 3G Systems.

https://doi.org/10.1017/S1759078724001223 Published online by Cambridge University Press